ARCHIVES OF BIOCHEMISTRY AND BIOPHYSICS
Vol. 333, No. 1, September 1, pp. 225–232, 1996
Article No. 0385

Visualization of the Reaction Layer in the Immediate Membrane Vicinity

Yuri N. Antonenko,[1] Peter Pohl,[2] and Eike Rosenfeld[3]
Medical Department, Institute of Medical Physics and Biophysics, Martin-Luther-University, 06097 Halle, Germany

Received April 1, 1996, and in revised form June 10, 1996

Coupled processes of diffusion and chemical reaction are quantitatively analyzed by means of proton concentration profile measurements in the immediate membrane vicinity. Because mass transfer across the unstirred layer (USL) is thought to proceed via diffusion, only the size of the USL is used as a scale for diffusion restrictions. Limitations associated with the finiteness of the reaction rate are characterized by the size of the reaction layer (RL). The latter is defined as the distance from the membrane where equilibrium is reached if transmembrane diffusion is followed by chemical reactions proceeding in the solution layers adjacent to the membrane. The well-known reaction of acetaldehyde oxidation catalyzed by alcohol dehydrogenase in the presence of NADH was selected because it is accompanied by an easily measurable alkalinization of the solution. The enzyme/coenzyme and the substrate were added to opposite sides of the membrane. A theoretical model describing the reaction and diffusion kinetics enabled us to calculate the size of the RL from the pH profile within the USL of a planar bilayer membrane showing a high proton permeability. As the enzyme concentration increased, the initially reaction-limited kinetics of the total turnover became diffusion limited under our experimental conditions due to a dramatic shortening of the RL.

Key Words: Unstirred layer; diffusion; bilayer; alcohol dehydrogenase; microelectrode.

A kinetic analysis of coupled processes of diffusion and chemical reaction is essential for the understanding of many biological processes. Important implications were made, e.g., for the endogenously produced messenger, nitric oxide, based on the finding of its diffusion span (1). Diffusive restrictions were identified as the limiting factor for numerous chemical reactions such as ligand–receptor interactions (2). Tissue respiration also can be limited by the delivery of oxygen to cells and mitochondria (3).

The rate of substrate transformation in the immediate membrane vicinity depends on the relative competition of reactivity and of the capability for diffusive flow. Along with a quantitative computational analysis made for some special systems (4, 5), empirical equations were introduced to characterize the interaction of diffusional transport and transformation reactions. Weisz (6) used a diffusion parameter, similar to the Thiele factor, to discriminate between the kinetic and the diffusion regimes of a catalytic reaction.

A quantitative description of the relative competition of diffusion and reaction becomes available also from the knowledge of the length of the unstirred and the reaction layers. Adjacent to the membrane, the existence of a completely unstirred region is assumed that yields abruptly to a perfectly stirred region. Within the unstirred layer (USL)[4] there is no convective mixing and movement takes place solely by diffusion. USLs play an important role in biological transport and accompanying transformation processes due to the existence of differences between the solute concentrations adjacent to the membrane and those in the bulk (7). In particular they are essential in some physiological processes, such as coupling of water transport in the lateral intercellular spaces of epithelia, or in the conservation of solutes transiently leaving the cell during an action potential (7). The presence of the USLs leads to an underestimation of the permeabilities of well permeable substances (8, 9). They play a unique role modi-

[1] Permanent address: Moscow State University, Belozersky Institute of Physico-Chemical Biology, 119899 Moscow, Russia.
[2] To whom the correspondence should be addressed. Fax +49 345 5571632. E-Mail: pohl@med-biophysik.uni-halle.d400.de.
[3] Permanent address: Fachhochschule Merseburg, Fachbereich Informatik und Angewandte Naturwissenschaften, Geusaer Str., 06127 Merseburg, Germany.

[4] Abbreviations used: USL, unstirred layer; RL, reaction layer; AlDH, alcohol dehydrogenase.

0003-9861/96 $18.00

fying the permeabilities of weak electrolytes through membranes of cells in suspension and in epithelial sheets (10). It was suggested that the thickness of the USL has a regulative function for the intestinal absorption (11).

Due to the substantial contribution to diffusion processes, the USLs affect the kinetics of chemical reactions near the membrane. The presence of USLs at adsorptive surfaces has been shown to distort the apparent kinetics of carrier-mediated transport systems (8, 12). Chemical transformations catalyzed by enzymes immobilized on the membrane surface may be diffusion controlled due to the existence of the USLs (13). Moreover, the kinetics of a subsequent chemical modification taking place in the immediate membrane vicinity after transmembrane substrate diffusion actually depends on the USL's thickness (14). This is true for the reversible dissociation of weak acids and bases as well as for catalytic reactions occurring due to the presence of bound or soluble enzymes (15, 4).

The term reaction layer (RL) was introduced to define the space where the chemical reactions are thought to take place (16). Within the RL reactants and reaction products are not in the equilibrium. It is assumed that equilibrium is reached in a distance from the interface which is larger than the thickness λ of the RL. The interfacial concentrations of the reactants and the reaction products may be calculated extrapolating their gradients at large distances if λ is much smaller than δ. This is true for the (de)protonization of weak acids and bases (16, 17) but cannot be assumed for other reactions, i.e., enzymatic ones.

In spite of its importance the width of the RL has not been measured for membrane systems yet. In addition, the interconnections between λ and other parameters describing a reaction-diffusion system have not been investigated. Here we report an experimental approach allowing the width of the RL to be measured in the immediate vicinity of planar bilayer lipid membranes.

The thickness of both the reaction and the unstirred layers may be obtained from the concentration distribution of the substrate or the product measured by means of microelectrode (18) or interferometrical techniques (19) in the solution layers adjacent to the membrane. In the present paper the reduction of acetaldehyde in the presence of alcohol dehydrogenase (AlDH) and NADH is studied with the help of pH microsensors adopted to planar bilayer membranes (20):

$$CH_3CHO + NADH + H^+ \rightleftharpoons CH_3CH_2OH + NAD^+. \quad [1]$$

If the substrate and the enzyme are separated by the membrane, nonmonotonic proton concentration profiles are obtained under certain conditions (21). From the bell-like shape of the profile the thickness of the reaction layer can be deduced only if the BLM is highly permeable not only to acetaldehyde and alcohol but to protons as well (Fig. 1). The nonmonotonic course of the pH profiles is analyzed by a simple theoretical model allowing us to describe the interconnection between diffusion and reaction.

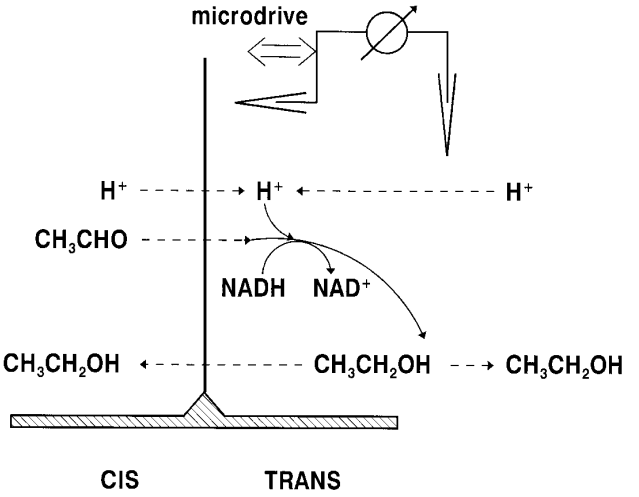

FIG. 1. The reaction of acetaldehyde oxidation catalyzed by alcohol dehydrogenase in the presence of NADH proceeds at the *trans* side. The enzyme/coenzyme and the substrate are added to opposite sides of the membrane. After the addition of acetate the membrane is highly permeable not only to acetaldehyde and alcohol but to protons as well. pH profiles within the unstirred layer near the planar bilayer lipid membrane are measured with the help of a microelectrode driven by a hydraulic microdrive.

THEORY

The unstirred layer is defined in terms of the concentration gradient at the membrane solution interface (22):

$$\frac{|c_s - c_b|}{\delta} = \left.\frac{\partial c}{\partial x}\right|_{x=0}, \quad [2]$$

where x is the distance from the membrane. c_s and c_b are the concentrations of the diffusing substances at the membrane surface and in the bulk solution, respectively. Within the USLs transport is thought to occur by diffusion only. Assuming an invariant diffusion coefficient, transport restrictions can be characterized by the size δ of the USL.

Reaction restrictions may be described in an analogous way by defining the thickness of the reaction layer. In the case of the transmembrane proton transport induced by a protonophore (16, 23) or by other weak acids and bases (17, 24, 25), the reaction layer

does not significantly affect the permeability data obtained. Theoretical considerations based on the knowledge of the protonation and dissociation rates shows that λ does not exceed a few nanometers (16, 17). In order to determine the bulk diffusion limitation of the H^+ ion conductance through a gramicidin channel, the effect of formic acid was investigated (26). From the kinetic model derived by Decker and Levitt (26) follows that λ is less than 1 nm. A different approach was reported by Gutknecht *et al.* (27) who investigated the transport of carbon dioxide through BLMs in the presence of carbon anhydrase. It was shown that an equilibrium state did not exist within the whole unstirred layer at low enzyme concentrations.

Thus the width of reaction layers in the systems studied was extreme; i.e., it was much less or much bigger than the width of the unstirred layer. It may be proposed that either equilibrium was established throughout the whole USL (in the first case) or that the concentration of the reaction product in the USLs was negligible (in the latter case). It should be pointed out that the theoretical analysis of systems of these kind (membrane, USLs, enzymatic reaction) was based on some substantial simplifications due to complexity of the system (15, 28). In addition, all these theoretical models used the conventional concept of the unstirred layer assuming an existence of a distinct boundary between a well-stirred bulk region and an unstirred near-membrane region. Because this gives the convenient opportunity to linearize the system, we were forced to use this concept in our theoretical analysis also. The main difference between the following theoretical treatment and those published earlier by LeBlanc (16) and Markin *et al.* (17) is that the condition $\lambda \ll \delta$ is absent now. In previous works it was necessary to estimate the concentrations of the permeating substance and the reaction product at the membrane/water interfaces by extrapolating their gradients at large distances (16). Due to the exact knowledge of the concentration profile from experimental measurements there is no need to hold this constraint any longer.

The starting point of all comparable theoretical models (16, 17) is the reaction equations combined with various simplifications. In the present model instead of the catalytic reaction (1) a reversible transformation of a substrate S into a product P which takes place in the immediate vicinity of the membrane at the trans side is considered.

$$S \underset{k_{-1}}{\overset{k_1}{\rightleftharpoons}} P. \qquad [3]$$

The experimental system is treated in a highly simplified manner; however, its most important features remain unaffected as will be shown under Discussion.

The membrane is assumed to be a barrier only for AlDH located at the *trans* side but S and P are able to permeate. Within the USL the substrate concentration s and the product concentration p are functions of the distance x from the membrane ($x = 0$) both at the trans ($\delta > x > 0$) and the *cis* sides ($-\delta < x < 0$). The thickness of the membrane is much smaller than δ and may be neglected. At the *cis* side s and p are determined by diffusion only:

$$D_S \frac{d^2s}{dx^2} = 0 \qquad [4]$$

$$D_P \frac{d^2p}{dx^2} = 0, \qquad [5]$$

where $s(-\delta) = S_0$ and $p(-\delta) = 0$.

At the *trans* side the diffusion and the chemical reaction as well have to be taken into account:

$$D_S \frac{d^2s}{dx^2} = k_1 s - k_{-1} p \qquad [6]$$

$$D_P \frac{d^2p}{dx^2} = -k_1 s + k_{-1} p, \qquad [7]$$

where $s(\delta) = p(\delta) = 0$. Additional boundary conditions may be found from the assumed infinite membrane permeability for S and P:

$$s_{x=-0} = s_{x=+0};\ p_{x=-0} = p_{x=+0} \qquad [8]$$

$$s'_{x=-0} = s'_{x=+0};\ p'_{x=-0} = p'_{x=+0}. \qquad [9]$$

For both, *cis* and *trans* sides the following differential equation holds:

$$D_S \frac{d^2s}{dx^2} + D_P \frac{d^2p}{dx^2} = 0. \qquad [10]$$

Consequently the sum of $s(x)$ and $p(x)$ must be a linear function of the type:

$$p(x) + s(x) = ax + b. \qquad [11]$$

The variables are now substituted for dimensionless quantities:

$$\bar{S} = \frac{s}{S_0};\ \bar{P} = \frac{p}{S_0};\ \xi = \frac{x}{\delta}. \qquad [12]$$

Assuming that the diffusion coefficients for the substrate and the product are equal the constants a and b can be found as $-S_0/2\delta$ and $S_0/2$ respectively from

the Eqs. [4]–[7], [11], and [12]. Now Eq. [11] can be rewritten as:

$$\bar{S} + \bar{P} = \frac{1}{2} - \frac{\xi}{2}. \qquad [13]$$

Inserting this solution into Eq. [7] we find

$$\frac{d^2\bar{P}}{d\xi^2} - (\alpha^2 + \beta^2)\bar{P} = -\frac{\alpha^2}{2}(1 - \xi),$$

where

$$\alpha^2 = \frac{\delta^2 k_1}{D}; \beta^2 = \frac{\delta^2 k_{-1}}{D} \qquad [14]$$

with the boundary condition $\bar{P}(1) = 0$.

From Eq. [5] follows that $\bar{P}(\xi)$ is a linear function in the interval $-1 \leqslant \xi \leqslant 0$ and can be written in the form:

$$\bar{P}(\xi) = e\xi + g. \qquad [15]$$

The boundary condition $\bar{P}(-1) = 0$ gives $e = g$. It means that the first derivation of $\bar{P}(\xi)$ is equal to $\bar{P}(\xi)$ itself at the point $\xi = 0$. Using Eq. [9] the same holds for the *trans* side:

$$\bar{P}'(0) = \bar{P}(0). \qquad [16]$$

It should be pointed out that it is this equation that leads to the appearance of the maximum on the distribution of $\bar{P}(\xi)$. In fact Eq. [16] means that the product concentration increases with the distance from the membrane at low distances. From $\bar{P}(1) = 0$ follows that $\bar{P}(\xi)$ has a maximum between 0 and 1. This corresponds well to the appearance of the maximum on the experimental pH profiles after the induction of the proton permeability of the membrane by the addition of high acetate concentration at both sides of the membrane (Fig. 4). With Eq. [16] the differential Eq. [14] can easily be solved:

$$\bar{P} = A_1 e^{\gamma\xi} + A_2 e^{-\gamma\xi} + \frac{\alpha^2}{2\gamma^2}(1 - \xi)$$

with

$$\gamma^2 = \alpha^2 + \beta^2 \qquad [17]$$

$$A_1 = \frac{\alpha^2}{\gamma^2(\gamma + \gamma e^{2\gamma} + e^{2\gamma} - 1)}, A_2 = -A_1 e^{2\gamma}.$$

The back transformation of the dimensionless variable ξ into x gives the parameter δ/γ called thickness of the reaction layer λ. This terminology is in agreement with that introduced by LeBlanc (16). In the space between the membrane and λ the catalytic reaction is assumed to be not in equilibrium. At a distance between λ and δ the profile is determined by diffusion and the equilibrium constant only.

MATERIALS AND METHODS

The BLMs are formed by a conventional method (29) in a hole, 1.2 mm in diameter, in the center of a PTFE diaphragm dividing a chamber into two compartments. The membrane forming solutions contains 20 mg phosphatidylcholine from soybeans (Sigma; Deisenhofen, Germany) and 10 mg cholesterol (Serva; Heidelberg, Germany) in 1 ml of *n*-decane (Merck; Darmstadt, Germany). The bathing solution consists of 1 mM Tris (Fluka; Neu-Ulm, Germany), 3 mM NADH (Fluka), 2 mM dithioerythritol (Aldrich; Steinheim, Germany), 2 mM EDTA (Merck), and 100 mM KCl (Merck). It is agitated by magnetic bars with the same velocity in all experiments.

Alcohol dehydrogenase (470 U/mg protein, Fluka) is added to the *trans* side of the membrane at various concentrations (see legends to the figures). In order to prevent enzyme inactivation caused by contaminations of the samples of NADH, 2 mM dithioerythritol and 2 mM EDTA were added to the buffer solutions. pH of the buffer is 7.5. The activity of the enzyme is monitored via the proton concentration shifts induced in a solution of 3 mM NADH and 4 mM acetaldehyde (Merck). It is equal to 1.2 μmol H^+/min/μg protein.

Acetaldehyde is added to the *cis* compartment. The catalytic reaction proceeding at the *trans* side due to the presence of AlDH brings about a concentration gradient of protons within the USL (30). This gradient is measured in terms of a potential difference between a pH microelectrode and a reference electrode, also placed in the buffer solution at the *trans* side of the membrane (31, 32). The voltages are recorded every second by a Keithley 617 electrometer (Keithley Instruments; Cleveland, OH) and transferred to a personal computer via an IEEE interface (Keithley Instruments; Taunton, MA). The control of the measuring device, data collection, and analysis are performed with the help of the software package Asyst (Asyst Software Technologies; Rochester, NY).

The pH sensors are made of glass capillaries containing antimony. After pulling their tips have a diameter of about 5 μm. The 90% response time of the microelectrode is less than 1 s. It is moved with a velocity of 2 μm s^{-1} perpendicularly to the surface of the BLM by means of a hydraulic microdrive manipulator (Narishige; Tokyo, Japan). The diameter of the electrode is two orders of magnitude smaller than that of the membrane. Artifacts due to a very slow electrode movement are therefore unlikely. Nevertheless, possible effects of time resolution or distortion of the USL are tested by making measurements while moving the microelectrode toward and away from the bilayer. Because no hysteresis is found, it can be assumed that an electrode of appropriate time resolution is driven without any effect on the USL.

All distance measurements are made relatively to the membrane. The touching of the membrane is indicated by the appearance of a small spot in the middle of the black membrane that is observed with the help of a microscope. Alternatively, the onset of a steep potential change that usually accompanies the touching of the membrane can be taken as the reference position for the membrane surface (20). However, the faster optical method is preferable because it helps to avoid membrane rupture. The accuracy of the distance measurements was estimated to be ± 5 μm.

RESULTS

Figure 2 shows the pH profiles near a BLM induced by the addition of an increasing concentration of alcoholdehydrogenase. AlDH is given to the *trans* com-

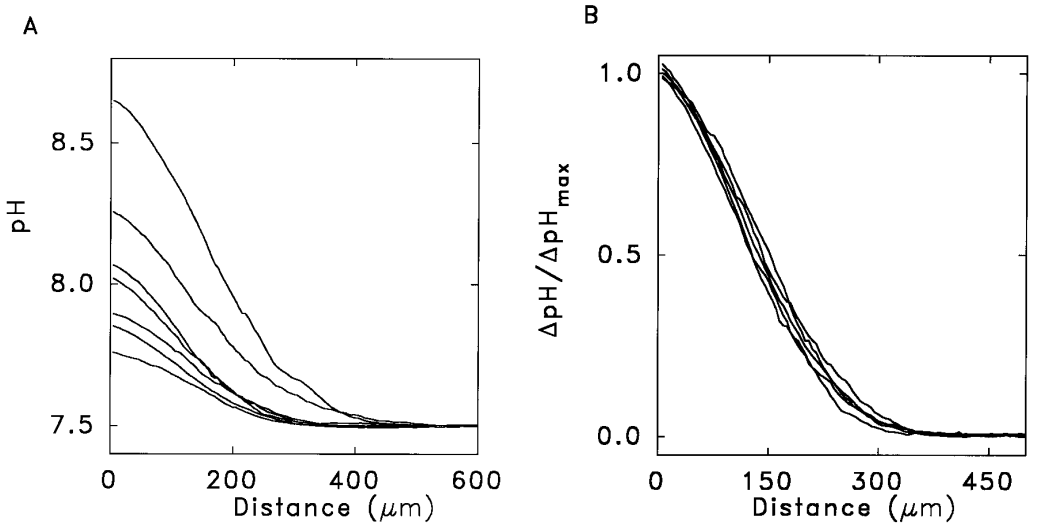

FIG. 2. (A) Series of steady-state pH profiles near a BLM induced by acetaldehyde permeation and alcohol dehydrogenase (AlDH) functioning. Acetaldehyde (4 mM) was added to the *cis* side and different AlDH concentrations (from lower to upper plot: 0.5, 1, 1.5, 2.5, 3.5, 5.5, and 11 μg/ml) to the *trans* side. (B) The profiles indicated in A are replotted in B in terms of the ratio of the actual pH shift ($\Delta pH = pH[0] - pH[x]$) and the maximum pH shift ($\Delta pH_{max} = pH[0] - pH[\infty]$).

partment. Acetaldehyde added to the *cis* side permeates through the membrane and is reduced due to the presence of enzyme and coenzyme (NADH) at the *trans* side. This reaction is accompanied by the alkalinization of the solution layer adjacent to the membrane. The profiles indicated in Fig. 2A are replotted in Fig. 2B in terms of the ratio of the actual pH shift at the distance x and the maximal pH shift. Within the experimental error the profiles of part B coincide. In the absence of a protonophore the pH profiles do not reflect the spatial rate distribution of the reaction [1].

In a subsequent experiment the membrane is permeabilized for protons by the addition of equal amounts of sodium acetate to the buffer solutions at both sides of the membrane. No net proton flux is induced under the conditions of a zero transmembrane acetate gradient. A series of pH profiles is recorded in the presence of 150 mM acetate in the buffer solutions (Fig. 3). These profiles have a maximum at low enzyme concentrations indicating that the reaction of proton consumption runs at a measurable distance from the membrane. This distance is a function of the enzyme concentration. At a low rate of the enzymatic reaction, acetaldehyde must cross a long distance before it can be reduced by NADH. The maximum is shifted toward the membrane at high enzyme concentrations (Fig. 3).

In spite of the high acetate concentrations, the pH values at both sides of the membrane are not equal (Fig. 3). Higher amounts of acetate and the addition of CCCP and valinomycin do not lead to a further decrease of the proton concentration gradient across the membrane (data not shown).

A relevant quantitative analysis of the concentration profiles should be carried out keeping the pH dependence of the catalytic reaction in mind. For that purpose the experiments of Fig. 3 are repeated at a buffer capacity 10-fold increased (Fig. 4). Under these conditions the transmembrane pH gradient is small. The standard deviation of the position of the profile maxi-

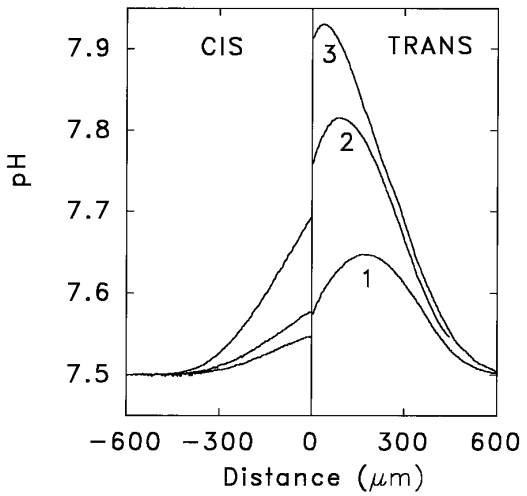

FIG. 3. Series of steady-state pH profiles near a BLM measured in the presence of 150 mM sodium acetate in the *trans* and *cis* solutions. Acetaldehyde (4 mM) was added to the *cis* side and AlDH in different concentrations to the *trans* side: (1) 2 μg/ml, (2) 4 μg/ml, and (3) 33 μg/ml.

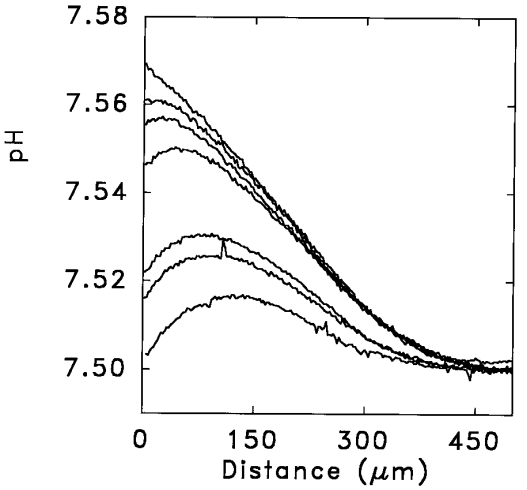

FIG. 4. Steady-state pH profiles near a BLM measured in the presence of 150 mM sodium acetate and 10 mM Tris in the solution. Acetaldehyde (4 mM) was added to the *cis* side and different AlDH concentrations (4, 6.5, 10, 20, 33, 66, and 140 μg/ml from lower to upper plot) to the *trans* side.

mum and of the size of the concentration boundary layer does not exceed 11 μm. Variations of the pH shift are lower than 7%.

DISCUSSION

Direct evidence was found that the boundary layer in the immediate vicinity of a porous enzymatic surface should be taken into account not only as a "... diffusional barrier, but essentially as a new compartment in which the high product concentration level governs its own distribution on both sides of the membrane" (4). In order to compare the theoretical predictions and the experimental results the variables pH and x should be transformed into $\bar{P}$ and ξ. The shapes of proton and product concentration profiles are assumed to be identical but with different signs.

$$\bar{P}(\xi) = \frac{p(x)}{S_0} \propto \left(1 - \frac{[H^+](x)}{[H^+]_0}\right). \qquad [18]$$

Using [17] and [18] in the following form

$$\bar{P}(\xi) = \frac{\alpha^2 e^{2\gamma - x\gamma/\delta} - \alpha^2 e^{x\gamma/\delta}}{-\gamma^2 + \gamma^3 + (1+\gamma)\gamma^2 e^{2\gamma}} + \frac{\alpha^2 \frac{x}{\delta}}{2\gamma^2} - \frac{\alpha^2}{2\gamma^2} \qquad [19]$$

the experimental pH profiles can nicely be fitted. The profile calculated with the help of the parameters α, γ, and δ coincides with the experimental profile. Figure 5 shows the fitted curves for the experiments of Fig. 4. The theoretical model describes well the behavior of the experimental system in spite of the simplifications made. Deviations from a monotonic profile course are correctly predicted by the model. Indeed, if the enzyme concentration is small, i.e., at low reaction rates, the equilibrium distance is large. The opposite situation is observed at high enzyme concentrations—the concentration profile is not distinguishable from profiles obtained under the conditions of simple diffusion (31, 32), i.e., λ is below the measurement accuracy. However, for low enzyme concentrations the fitting is unsatisfactory. Obviously, the theoretical model is not applicable for very low reaction rates. This is not surprising in view of the assumptions made. The chemical reaction is treated as the transformation of one substrate into one product (Eq. [2]), whereas reaction [1] is much more complicated. Furthermore, the catalytic character of the reaction was neglected. Even for the simple reaction [2] the rate in the presence of an enzyme should be treated in the following way (33)

$$E + S \underset{l_{-1}}{\overset{l_1}{\rightleftharpoons}} ES \underset{l_{-2}}{\overset{l_2}{\rightleftharpoons}} E + P \qquad [20]$$

$$v = \frac{dp}{dt} = \frac{(l_1 l_2 s - l_{-1} l_{-2} p) E_0}{l_1 s + l_{-2} p + (l_{-1} + l_2)}, \qquad [21]$$

where E_0 is the sum of the bound and the free enzyme concentrations. Furthermore, buffer effects are neglected, although the proton concentration is used to study the system. Moreover, according to the unstirred layer model a linear dependence of the concentration

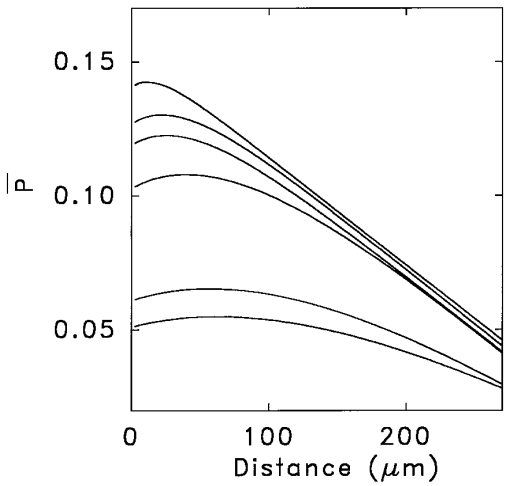

FIG. 5. Fitted curves for the experimental profiles of Fig. 3 (AlDH concentrations from lower to upper curve: 6.5, 10, 20, 33, 66, and 140 μg/ml). The transformations were made with the help of the theoretical model (Eq. [18]).

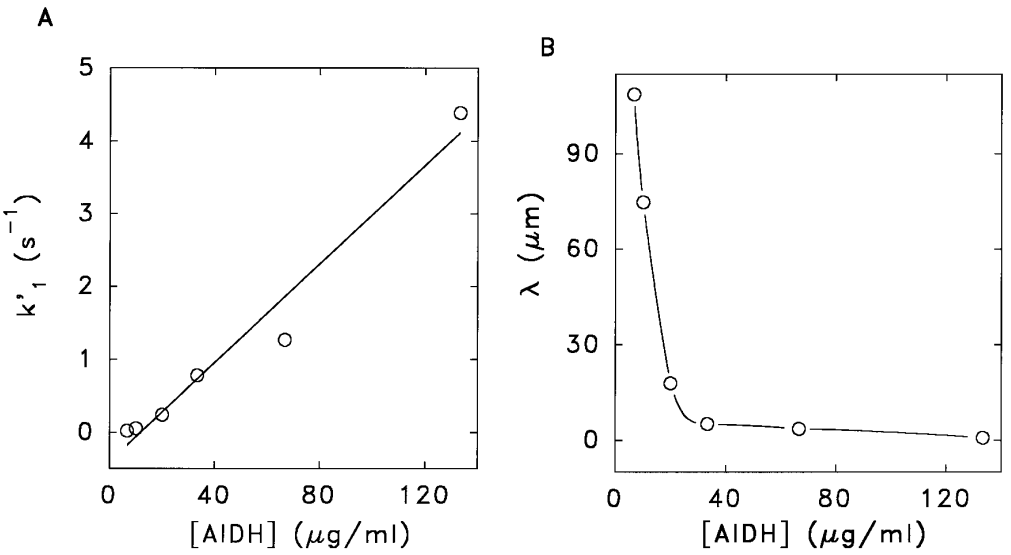

FIG. 6. The enzyme concentration determines (A) the reaction rate and (B) the width of the reaction layer. Both parameters are calculated from the experiments of Fig. 3 (Eq. [18]). k'_1 is proportional to the reaction rate k_1 describing the forward transformation rate of the substrate S into the product P.

on the distance from the membrane is assumed instead of an exponential one (32).

Both the size of the concentration boundary layer δ and the width of the reaction layer λ ($\lambda = \delta/\gamma$) are calculated from the experimental profiles with the help of an iteration algorithm based on Eq. [18]. Figure 6 reflects the dependence of the width of the reaction layer and of the reaction rate on the enzyme concentration. The value of the proton concentration shift in the immediate vicinity of the membrane depends on the buffer capacity. Therefore, the reaction rates k_1 and k_{-1} cannot be deduced from α and γ. The values k'_1 and k'_{-1} which are proportional to k_1 and k_{-1} respectively are used instead. Because k'_1 and k'_{-1} increase linearly with an increase in the enzyme concentration (Fig. 6A), k_1 and k_{-1} are expected to do the same. This behavior is in agreement with the theoretical predictions of Eq. [20]. An additional support for the validity of the simple model is the behavior of the thickness of the USL. δ should remain constant since the stirring conditions are invariant. Indeed, δ is calculated to be 379 ± 8 μm.

The concentration distributions of reactants and reaction products in the immediate membrane vicinity were analyzed in the past by LeBlanc (16) and Markin *et al.* (17). Both of them analyzed the kinetics of diffusion and dissociation of a weak acid. Because the thickness of the reaction layer was evaluated to be much smaller than the size of the ULS, the near-membrane concentrations were found by extrapolation of the concentration gradients at large distances. In the present study it has been possible to measure the concentration profile within the reaction layer because the velocities of the chemical transformation chosen and those of the diffusion of the reactants involved are comparable. From the shape of the concentration distribution we have calculated the thickness of the RL. The hyperbolic behavior of $\lambda(E_0)$ is in agreement with our theoretical model. If the enzyme concentration is very low, then the RL is comparable with the USL. Under these conditions alterations of λ caused by an increase in the reaction rate are not measurable. The same holds for very high reaction rates when the reaction layer is not distinguishable from the membrane surface. Between these extreme cases the thickness of the reaction layer strongly depends on the enzyme concentration (Fig. 6B). Transmembrane substrate diffusion followed by catalytic transformation and product diffusion are characterized in a simple mathematical model that reflects the main features of the experimental system. The parameters thickness of the unstirred and reaction layers may be very useful to describe the competition between reactivity and diffusive flow.

ACKNOWLEDGMENT

This work was supported by the Deutsche Forschungsgemeinschaft (Ro 1057/2-1).

REFERENCES

1. Lancaster, J. R. (1994) *Proc. Natl. Acad. Sci. USA* 91, 8137–8141.
2. Wang, D., Gou, S. Y., and Axelrod, D. (1992) *Biophys. Chem.* 43, 117–137.
3. Riley, M. R., Buettner, H. M., Muzzio, J., and Reyes, S. C. (1995) *Biophys. J.* 68, 1716–1726.
4. Maisterrena, B., Blum, L. J., and Coulet, P. R. (1987) *Biochem. J.* 242, 835–839.

5. Glaser, R. W. (1993) *Anal. Biochem.* 213, 152–161.
6. Weisz, P. W. (1973) *Science* 179, 433–440.
7. Barry, P. H., and Diamond, J. M. (1984) *Physiol. Rev.* 64, 763–872.
8. Wilson, F. A., and Dietschy, J. M. (1974) *Biochim. Biophys. Acta.* 373, 112–126.
9. Walter, A., and Gutknecht, J. (1986) *J. Membr. Biol.* 90, 207–217.
10. Jackson, M. (1987) *in* Membrane Physiology (Andreoli, T. E., and Hoffmann, J. F., Eds.), pp. 235–247, Plenum, New York.
11. Levitt, M. D., Strocchi, A., and Levitt, D. G. (1992) *Am. J. Physiol.* 262, G593–G596.
12. Preston, R. L. (1982) *Biochim. Biophys. Acta* 688, 422–428.
13. Kasche, V., and Kuhlmann, G. (1980) *Enzyme Microb. Technol.* 2, 309–312.
14. Winne, D. (1973) *Biochim. Biophys. Acta* 298, 27–31.
15. Wingard, L. B., Katchalski-Katzir, E., and Goldstein, L. (1976) Applied Biochemistry and Bioengineering. Vol. 1. Immobilized Enzyme Principles. Academic Press, New York.
16. LeBlanc, O. H. (1971) *J. Membr. Biol.* 4, 227–251.
17. Markin, V. S., Portnov, V. I., Simonova, M. V., Sokolov, V. S., and Cherny, V. V. (1987) *Biol. Membr.* 4, 502–523. [In Russian]
18. Lucas, M. L., Schneider, W., Haberich, F. J., and Blair, J. A. (1975) *Proc. R. Soc. London Ser. B* 192, 39–48.
19. Lerche, D. (1976) *J. Membr. Biol.* 27, 193–205.
20. Antonenko, Y. N., and Bulychev, A. A. (1991) *Biochim. Biophys. Acta* 1070, 279–282.
21. Antonenko, Y. N., and Pohl, P. (1995) *Biochim. Biophys. Acta* 1235, 57–61.
22. Dainty, J., and House, C. R. (1966) *J. Physiol.* 182, 66–78.
23. McLaughlin, S. G. A., and Dilger, J. P. (1980) *Physiol. Rev.* 60, 825–863.
24. Gutknecht, J., Bruner, L. J., and Tosteson, D. C. (1972) *J. Gen. Physiol.* 59, 486–502.
25. Gutknecht, J., and Tosteson, D. C. (1973) *Science* 182, 1258–1261.
26. Decker, E. R., and Levitt, D. G. (1988) *Biophys. J.* 53, 25–32.
27. Gutknecht, J., Bisson, M. A., and Tosteson, D. C. (1977) *J. Gen. Physiol.* 69, 779–794.
28. Murray, J. D. (1977) Lectures on Nonlinear-Differential-Equations. Models in Biology, Clarendon Press, Oxford.
29. Mueller, P., Rudin, D. O., Tien, H. T., and Wescott, W. C. (1963) *J. Phys. Chem.* 67, 534–535.
30. Antonenko, Y. N., and Yaguzhinsky, L. S. (1986) *Biochim. Biophys. Acta* 861, 337–344.
31. Antonenko, Y. N., Denisov, G. A., and Pohl, P. (1993) *Biophys. J.* 64, 1701–1710.
32. Pohl, P., Antonenko, Y. N., and Rosenfeld, E. (1993) *Biochim. Biophys. Acta* 1152, 155–160.
33. Bisswanger, H. (1994) Enzymkinetik. Theorie und Methoden, pp. 92–94, VCH Verlagsgesellschaft mbH, Weinheim.